

# Performance characteristic of energy selective electron (ESE) refrigerator with filter heat conduction

Zemin Ding, Lingen Chen\*, and Fengrui Sun  
Postgraduate School, Naval University of Engineering,  
Wuhan 430033, P.R. China,  
Fax: 0086-27-83638709, Tel: 0086-27-83615046,  
e-mail: lgchenna@yahoo.com; lingenchen@hotmail.com

Recibido el 9 de marzo de 2009; aceptado el 11 de enero de 2010

The cooling load and coefficient of performance (COP) characteristic of an energy selective electron (ESE) refrigerator with filter heat conduction operating in the maximum cooling load regime and the intermediate regime (*i.e.* between maximum cooling load operation and reversible operation) are analyzed in this paper. In the analyses, the analytical formulae for cooling load and COP of the ESE refrigerator are derived for the two operation regimes, respectively. The performance characteristics are obtained by numerical calculations. The influence of the resonance widths on the performance of the ESE refrigerator in the intermediate regime is discussed. It is shown that, in the maximum cooling load operation regime, when the filter heat transfer is taken into account, the cooling load versus COP characteristic change from monotonic curves (without filter heat conduction) to parabolic-like ones (with filter heat conduction); while in the intermediate regime, the cooling load versus COP characteristic are always loop-shaped ones and the heat conduction of the filter does not change the shape of the characteristic curves. The cooling load is a parabolic-like function of resonance width while the COP is a monotonic one of resonance width. With the increase in thermal conductivity, the COP decreases in both operation regimes. The results obtained herein have theoretical significance for the understanding of thermodynamic performance of the micro-nano devices.

**Keywords:** Energy selective electron (ESE) refrigerator; cooling load; COP; performance characteristic.

Se analizan en este trabajo la carga de enfriamiento y el coeficiente de desempeño (COP, por sus siglas en inglés) de un refrigerador de selección de energía electrónica (ESE, por sus siglas en inglés), con filtro de conducción de calor, operando en el régimen de máxima carga de enfriamiento y en el régimen intermedio (*i.e.* entre la operación a máxima carga de enfriamiento y la operación reversible). Se deducen analíticamente fórmulas para la carga de enfriamiento y el COP del refrigerador ESE, bajo los dos regímenes de operación, respectivamente. Se obtienen, mediante cálculos numéricos, las características de funcionamiento. Se discute la influencia de los anchos de resonancia en el desempeño del refrigerador ESE en el régimen intermedio. Se demuestra que, en el régimen de operación a máxima carga de enfriamiento, cuando se toma en cuenta el filtro de transferencia de calor, la carga de enfriamiento versus el COP cambia de una curva monótona (sin filtro de calor de conducción) a curvas de tipo parabólico (con filtro de calor de conducción); en cambio, en el régimen intermedio, la carga de enfriamiento versus el COP son siempre curvas en forma de bucle y la conducción de calor del filtro no cambia la forma de las curvas características. La carga de enfriamiento es una función en forma de parábola del ancho de resonancia, mientras que el COP es una función monótona del ancho de resonancia. El COP decrece en ambos regímenes de operación, al aumentar la conductividad térmica. Los resultados que aquí se obtienen son teóricamente significativos para la comprensión del desempeño termodinámico de micro-nano dispositivos.

**Descriptores:** Refrigerador de selección de energía electrónica; carga refrigerante; COP; desempeño característico.

PACS: 84.50.+d; 05.70.Ln; 84.30.Vn; 05.40.Jc

## 1. Introduction

The energetics of electronic systems is interesting. Under certain conditions, electronic systems can behave as heat engines, refrigerators or heat pumps, including thermoelectric power generators and refrigerators [1-6], thermionic power generators and refrigerators [7-16], Brownian motors [17-23], and so on. Heat transfer is achieved by moving high energy electrons from one reservoir to the other for the thermoelectric and thermionic systems, and all the devices use barriers or other energy selection mechanisms such as resonant tunneling to limit the current flowing in the device to electrons within particular energy ranges [24,25]. On the other hand, a Brownian motor uses temperature differential [26,27] as the source of non-equilibrium to power a ratchet, which combines asymmetry with non-equilibrium process to generate directed particle motion.

A quantum ratchet [28-34] is another analogous mechanism, Reimann *et al.* [28,29] made a theoretical prediction about the existence of the temperature dependent net current reversal for quantum particles in a rocked ratchet, and it was observed in the experiment by Linke *et al.* [30] for electrons in the ballistic transport regime. Two models of the quantum ratchet were proposed by Yukawa *et al.* [31]. The quantum ratchet phenomenon of quantum point contacts was studied by Khrapai *et al.* [32,33]. Hoffmann and Linke [34] found that a two-terminal quantum dot bridging a temperature difference can operate as a thermometer by probing the Fermi-Dirac distributions of the electron gas on both sides of the quantum dot and they discussed the three different operation regimes of the device. Based on the experimental work [30,35-37] on the quantum ratchet, Humphrey *et al.* [38] and Linke *et al.* [39,40] investigated the behavior of the quantum ratchet acting as a heat pump. Further,

Humphrey *et al.* [41] proposed a novel mechanism of the quantum Brownian engine model for electrons. This mechanism combines the energy selective property of thermoelectric and thermionic systems with the temperature differential driving property of Brownian engines, and it was termed an energy selection electron (ESE) engine [42]. The ESE engine utilizes a temperature difference between two electron reservoirs to transport high energy electrons against an electrochemical potential gradient. The electrons are transported between the two reservoirs through an energy filter, which freely transmits electrons in a specified energy range and blocks the transport of all others. Depending on the direction of electron transportation, the ESE engine could behave as a refrigerator or heat engine. It was shown that the ESE refrigerator and heat engine could operate reversibly when the energy of the filter was suited at which the Fermi distributions in the two reservoirs had the same value [41]. This was called the reversible regime of operation of the ESE engine.

In the past 30 years, much progress has been made in the analyses of conventional macroscopic energy conversion systems using the theory of finite time thermodynamics (FTT) [43-52]. Recently, the method of FTT has also been used to analyze the optimum performance of microscopic systems such as the Brownian ratchet [53-57], the quantum ratchet [58] and electron engines [42,59] Velasco *et al.* [53] and Tu [54] studied the optimal performance of the Feynman engine using the theory of FTT. And the optimum performance of thermal Brownian motors was also investigated by some authors [55-57]. Esposito *et al.* [58] identified the operational conditions for maximum power of a nanothermoelectric engine consisting of a quantum dot embedded between two leads at different temperatures and chemical potentials, and found that the thermoelectric efficiency at maximum power agrees with the expression for Curzon-Ahlborn efficiency [59] up to quadratic terms. Humphrey [42] analyzed the optimal performance of the ESE refrigerator operating in the maximum cooling load regime and the intermediate operation condition (*i.e.* between the maximum cooling load operation and the reversible operation), respectively. He *et al.* [60] studied the optimum performance of an ESE refrigerator with heat leaks in the intermediate operation regime

Such energy selective systems are of theoretical significance to thermionic devices, such as thermionic refrigerators and power generators. Thermionic refrigerators and power generators are actually energy selective systems, for they utilize an energy barrier to selectively transmit high energy electrons ballistically between reservoirs. Because of the lack of a kind of barrier material with a sufficiently low work function [7,8], traditional thermionic devices with macroscopic gaps between emitter and collector plates are limited to very high temperature applications. Nanostructures are being investigated in an attempt to develop thermionic devices that can refrigerate or generate power at a low temperature [9,10], and successful solid-state thermionic cooling of up to a few degrees has been reported [61,62]. The transmission of electrons in these nanostructure devices share the same way as

the ESE system discussed in this paper. The results obtained in Refs. 41 and 42 in regard to the ESE systems have already been applied to the studies of thermoelectric and thermionic systems [14,15,63-67].

Previous research [68-70] has shown that the heat conduction by the barrier material is of great importance for the performance of electron energy devices, such as thermoelectric and thermionic refrigerators and power generators. However, results about the ESE refrigerator model in Refs. 41 and 42 are obtained without considering the heat conduction due to the propagation of phonons. Thus, based on Refs. 41 and 42, a further step made in this paper is to take into account the heat conduction of the energy filter via phonons for the ESE refrigerator, and to analyze its overall cooling load and COP characteristic. In the analyses, performance of the refrigerator operating in the maximum cooling load regime and the intermediate regime are discussed, respectively. The influence of the resonance widths on the cooling load and COP performance of the ESE refrigerator in the intermediate regime is discussed. Numerical examples show that when the filter heat transfer is taken into account, the characteristic of cooling load versus COP will change from monotonic ones to parabolic-like ones in the maximum cooling load regime, while in the intermediate regime, the curves of cooling load versus COP are always loop-shaped ones, and with the increase in thermal conductivity, the COP decreases in both operation regimes.

## 2. Model of ESE refrigerator

Figure 1 shows the schematic diagram of an ESE refrigerator with filter heat transfer via phonons. It consists of two infinitely large electron reservoirs and an energy filter. The two reservoirs have different temperatures and chemical

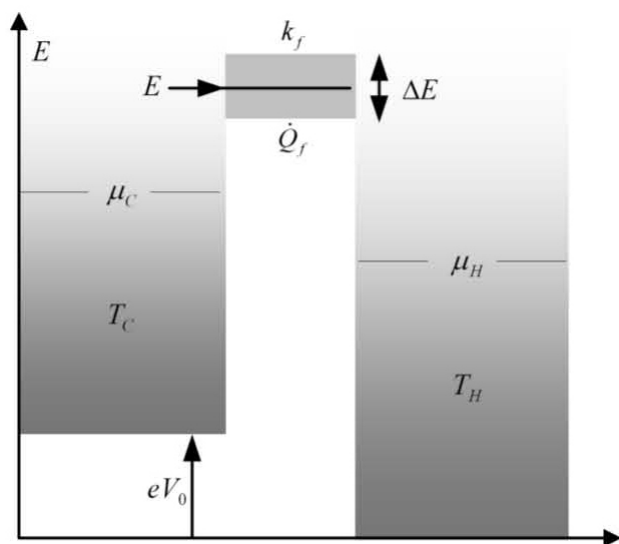


FIGURE 1. Schematic diagram of the ESE refrigerator with filter heat conduction via phonons.

potentials, where  $T_C$  and  $T_H$  are the temperatures of cold and hot reservoirs, and  $\mu_C$  and  $\mu_H$  are the chemical potentials of cold and hot reservoirs. They interact with each other only via the energy filter which freely transmits electrons with a specified range of energies. Meanwhile, the filter itself has a thermal conductivity  $k_f$  due to the propagation of phonons and contributes to the heat transfer between the two reservoirs. In Fig. 1,  $E$  is the central energy and  $\Delta E$  is the energy range of the electrons transmitted through the filter, and  $eV_0$  is a bias voltage that is applied to the hot reservoir.

According to the above description for the model, one can conclude that the heat transfer between the two reservoirs consists of two parts: one is the heat that is transferred by the electrons transmitted through the filter, and the other is that transferred by the filter itself via the transport of phonons.

Over an infinitesimal energy range  $\delta E$ , the rate of the received heat of the hot reservoir and the rate of released heat of the cold reservoir by the transmitted electrons are [41,42]

$$\dot{q}_{He} = \frac{2}{h}(E - \mu_H)(f_C - f_H)\delta E \quad (1)$$

$$\dot{q}_{Ce} = \frac{2}{h}(E - \mu_C)(f_C - f_H)\delta E \quad (2)$$

where  $h$  is Plank constant,  $f_C$  and  $f_H$  the Fermi distributions of electrons in the cold and hot reservoirs,

$$f_C = \frac{1}{1 + e^{(E - \mu_C)/(kT_C)}} \quad (3)$$

$$f_H = \frac{1}{1 + e^{(E - \mu_H)/(kT_H)}}$$

where  $k$  is Boltzman's constant.

While the rate of heat transferred from the hot reservoir to the cold reservoir by the filter itself is

$$\dot{Q}_f = k_f(T_H - T_C) \quad (4)$$

Equation (4) is similar to the bypass heat leakages of a conventional heat engine [71] and refrigerator [72] provided by Bejan [71,72].

According to Ref. 41, the ESE refrigerator could operate reversibly when the energy of the filter is suited to  $E_0 = (T_H\mu_C - T_C\mu_H)/(T_H - T_C)$ , at which the Fermi distributions in the reservoirs have the same value. The transfer of electrons in this condition will not result in an increase in the entropy of the system. This is the reversible operation regime of the ESE refrigerator.

### 3. Performance in the maximum cooling load operation regime

It is shown in Ref. 42 that, in the energy range of  $\mu_C < E < E_0$ , electrons contribute positively to the refrigeration of the refrigerator. So, in order to get the maximum cooling load, only electrons with energies between  $\mu_C$  and  $E_0$  should participate in the transport, and all others should be blocked. Thus, the rates of heat transferred by electrons at maximum cooling load conditions are

$$\dot{Q}_{He} = \int_{\mu_C}^{E_0} \dot{q}_{He} = \frac{2}{h} \int_{\mu_C}^{E_0} (E - \mu_H)(f_C - f_H)dE \quad (5)$$

$$\dot{Q}_{Ce} = \int_{\mu_C}^{E_0} \dot{q}_{Ce} = \frac{2}{h} \int_{\mu_C}^{E_0} (E - \mu_C)(f_C - f_H)dE \quad (6)$$

Combining Eqs. (4) to (6) gives the total increased amount ( $\dot{Q}_H$ ) of heat of hot reservoir per unit time and the total lost amount ( $\dot{Q}_C$ ) of heat of cold reservoir per unit time

$$\dot{Q}_H = \dot{Q}_{He} - \dot{Q}_f, \quad \dot{Q}_C = \dot{Q}_{Ce} - \dot{Q}_f \quad (7)$$

Using the first law of thermodynamics and combining Eqs. (4) to (7), one can obtain the cooling load ( $R_m$ ) and COP ( $\varepsilon_m$ ) in this regime

$$R_m = \dot{Q}_C = \frac{2}{h} \left[ r_0 k^2 (T_C^2 - T_C T_H) \ln a + k^2 (T_H^2 - T_C^2) \left( \frac{1}{2} \ln^2 a + g(a) \right) + k^2 T_C^2 \left( \frac{1}{2} \ln^2 \frac{1}{2} + g\left(\frac{1}{2}\right) \right) - k^2 T_H^2 \left( \frac{1}{2} \ln^2 b + g(b) \right) \right] - k_f (T_H - T_C) \quad (8)$$

$$\varepsilon_m = \frac{R_m}{(\dot{Q}_H - \dot{Q}_C)} = \left\{ [r_0 k^2 (T_C^2 - T_C T_H) \ln a + k^2 (T_H^2 - T_C^2) \left( \frac{1}{2} \ln^2 a + g(a) \right) + k^2 T_C^2 \left( \frac{1}{2} \ln^2 \frac{1}{2} + g\left(\frac{1}{2}\right) \right) - k^2 T_H^2 \left( \frac{1}{2} \ln^2 b + g(b) \right)] - \frac{1}{2} h k_f (T_H - T_C) \right\} / \left\{ r_0 (k T_H - k T_C)^2 \ln a - r_0 k^2 (T_H - T_C) \left( T_H \ln b - T_C \ln \frac{1}{2} \right) \right\} \quad (9)$$

where  $r_0$ ,  $a$ ,  $b$  and the function  $g$  are defined, respectively, as

$$r_0 = \frac{\mu_C - \mu_H}{k(T_H - T_C)}, \quad a = \frac{e^{r_0}}{1 + e^{r_0}}, \quad b = \frac{e^{(\mu_C - \mu_H)/(kT_H)}}{1 + e^{(\mu_C - \mu_H)/(kT_H)}}, \quad g(x) = \int_{0.5}^x \frac{\ln t}{1 - t} dt \quad (10)$$

To illustrate the preceding analysis, numerical examples are provided. In the calculations, it is considered that  $T_H = 2K$  and  $T_C = 1K$ .

Figure 2 shows the effect of the filter heat conduction on the COP performance in the maximum cooling load regime. It can be seen that, when  $k_f = 0$ , the COP in the maximum cooling load regime is a monotonic function of  $r_0$  and tends to one-third of the Carnot value  $(1/3)T_C(T_H - T_C) = 1/3$  for small values of  $(\mu_C - \mu_H)$ ; when  $k_f = 1.0 \times 10^{-14}$  W/K, the characteristic curves of  $\varepsilon_m - r_0$  are parabolic-like ones and there exists a maximum COP ( $\varepsilon_{m,m}$ ) and the corresponding  $r_{0,\varepsilon_m}$ . The maximum value of COP decreases with the increase in filter heat conduction (*i.e.* the increase in thermal conductivity  $k_f$ ).

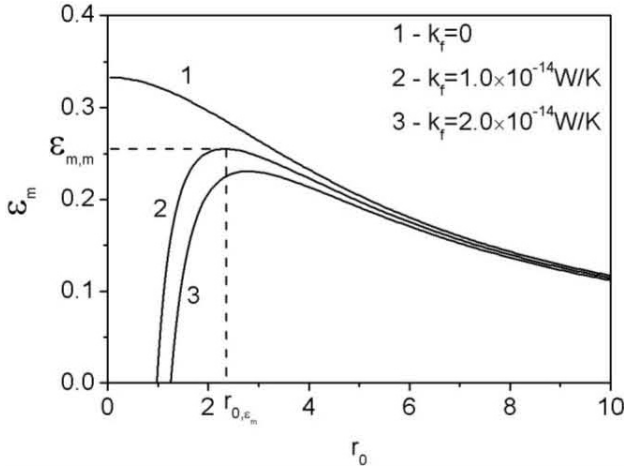


FIGURE 2. Influence of filter heat conduction on COP  $\varepsilon_m$  versus  $r_0$  characteristic in the maximum cooling load regime.

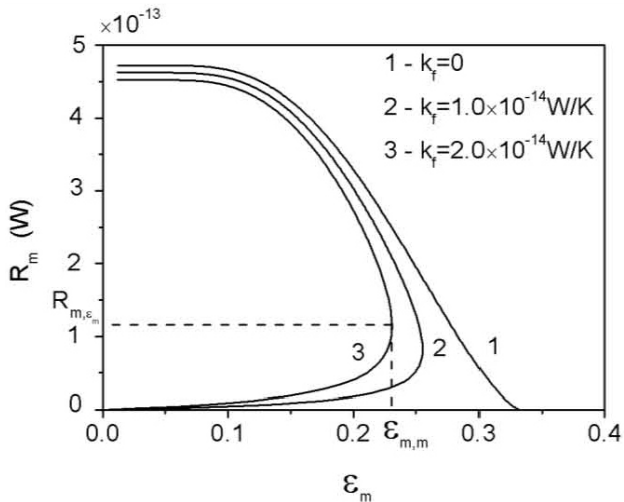


FIGURE 3. Influence of filter heat conduction on cooling load  $R_m$  versus COP  $\varepsilon_m$  characteristic in the maximum cooling load regime.

Figure 3 shows the cooling load ( $R_m$ ) versus COP ( $\varepsilon_m$ ) characteristic for the ESE refrigerator in the maximum cooling load regime. When there is no filter thermal conduction in the system ( $k_f = 0$ ), the curve of  $R_m - \varepsilon_m$  is a monotonic one, as shown by curve 1 in Fig. 3. When the filter thermal conduction is taken into account in the system, *i.e.*  $k_f = 1.0 \times 10^{-14}$  W/K and  $k_f = 2.0 \times 10^{-14}$  W/K, the curves of  $R_m - \varepsilon_m$  are parabolic-like ones, as shown by curves 2 and 3 in Fig. 3. There exists an optimum cooling load ( $R_{m,\varepsilon_m}$ ) which leads to the maximum COP ( $\varepsilon_{m,m}$ ). There are two different values of cooling load for a given COP and the refrigerator should work at the point where the cooling load is higher.

#### 4. Performance in the intermediate operation regime

In the intermediate operation regime, electrons with a finite energy range of  $\Delta E$  around central energy  $E$  are transmitted through the filter. The rates of heat transferred by electrons in the intermediate operation regime conditions are [42]

$$\begin{aligned} \dot{Q}_{He} &= \frac{2}{h} \int_{E-\Delta E/2}^{E+\Delta E/2} \dot{q}_{He} dE \\ &= \frac{2}{h} \int_{E-\Delta E/2}^{E+\Delta E/2} (E - \mu_H)(f_C - f_H) dE \end{aligned} \quad (11)$$

$$\begin{aligned} \dot{Q}_{Ce} &= \frac{2}{h} \int_{E-\Delta E/2}^{E+\Delta E/2} \dot{q}_{Ce} dE \\ &= \frac{2}{h} \int_{E-\Delta E/2}^{E+\Delta E/2} (E - \mu_C)(f_C - f_H) dE \end{aligned} \quad (12)$$

Combining Eqs. (4) and (11)-(12) gives the total increased amount ( $\dot{Q}_H$ ) of heat of hot reservoir per unit time as well as the total lost amount ( $\dot{Q}_C$ ) of heat of cold reservoir per unit time

$$\dot{Q}_H = \dot{Q}_{He} - \dot{Q}_f, \quad \dot{Q}_C = \dot{Q}_{Ce} - \dot{Q}_f \quad (13)$$

The cooling load ( $R_i$ ) and COP ( $\varepsilon_i$ ) of the ESE refriger-

ator operating in the intermediate regime are

$$R_i = \dot{Q}_C = \frac{2}{h} \int_{E-\Delta E/2}^{E+\Delta E/2} (E - \mu_C) \times (f_C - f_H) dE - k_f(T_H - T_C) \quad (14)$$

$$\varepsilon_i = R_i / (\dot{Q}_H - \dot{Q}_C) = R_i / \int_{E-\Delta E/2}^{E+\Delta E/2} 2(\mu_C - \mu_H) \times (f_C - f_H) / h dE \quad (15)$$

Also, numerical examples are provided to show the characteristic of the ESE refrigerator with the given values of temperatures and potential energy, *i.e.*  $T_H = 2$  K,  $T_C = 1$  K,  $\mu_C/k = 12$  K and  $\mu_H/k = 10$  K.

Figure 4 shows the cooling load ( $R_i$ ) versus COP ( $\varepsilon_i$ ) characteristic for the ESE refrigerator in the intermediate regime. It is considered that the resonance width  $\Delta E/k = 1$  K. One can see that the characteristic curves of  $R_i - \varepsilon_i$  are loop-shaped ones. For different thermal conductivities,  $k_f=0$ ,  $k_f=1.0 \times 10^{-14}$  W/K and  $k_f=2.0 \times 10^{-14}$  W/K, the COP decreases with the increase in filter heat transfer. The cooling load has a maximum ( $R_{i,m}$ )

with the corresponding COP ( $\varepsilon_{i,R_i}$ ). The COP also has a maximum ( $\varepsilon_{i,m}$ ) with the corresponding cooling load ( $R_{i,\varepsilon_i}$ ). The optimal regions of cooling load and COP for the refrigerator in the intermediate regime should be  $R_{i,\varepsilon_i} < R_i < R_{i,m}$  and  $\varepsilon_{i,R_i} < \varepsilon_i < \varepsilon_{i,m}$ .

Figure 5 shows the cooling load ( $R_i$ ) and COP ( $\varepsilon_i$ ) versus resonance width  $\Delta E/k$  characteristics in the intermediate regime. In the calculations, it is considered that  $k_f = 0$  and  $E/k = 13$  K. The characteristic curve of  $R_i - \Delta E/k$  is a parabolic-like one as shown by curve 1 in Fig. 5. There exists the optimum resonance width  $(\Delta E/k)_{R_i}$  leading to the maximum cooling load ( $R_{i,m}$ ). The characteristic curve of  $\varepsilon_i - \Delta E/k$  is a monotonic one as shown by curve 2 in Fig. 5, and the COP decreases with the increase of the resonance width  $\Delta E/k$ .

### 5. Conclusion

The cooling load and COP characteristic of the ESE refrigerator operating in the maximum cooling load regime and the

Nomenclature	
$E$	energy of electrons (J)
$eV_0$	bias voltage
$f$	Fermi distribution of electrons
$g$	a defined function
$h$	Plank constant
$k$	Boltzmann's constant
$k_f$	thermal conductivity of the filter (W/K)
$\dot{Q}$	rate of heat transfer (W)
$\dot{q}$	rate of heat transfer over a small energy range $\delta E$ (W)
$R$	cooling load (W)
$T$	temperature (K)
$\Delta E$	resonance width (J)
$\delta E$	a narrow energy range (J)
Greek symbols	
hline $\varepsilon$	coefficient of performance (COP)
$\mu$	chemical potential (J)
Subscripts	
$C$	cold electron reservoir
$C_e$	received heat of the cold reservoir
$f$	energy filter
$H$	hot electron reservoir
$H_e$	released heat of the hot reservoir
$i$	intermediate operation regime
$m$	maximum value/maximum cooling load operation regime

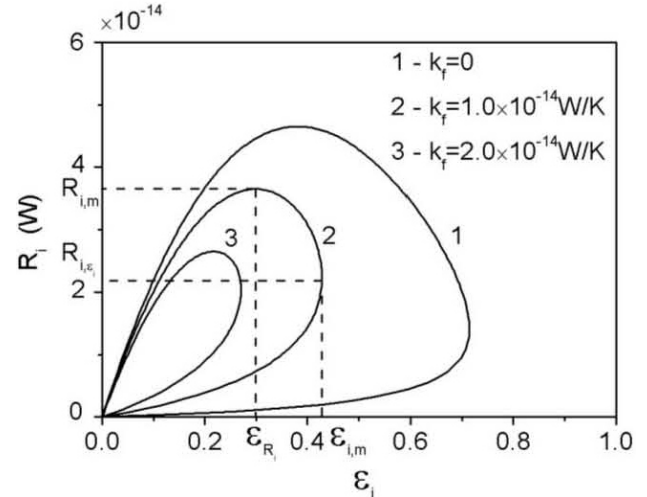


FIGURE 4. Influence of filter heat conduction on cooling load  $R_i$  versus COP  $\varepsilon_i$  characteristic in the intermediate regime.

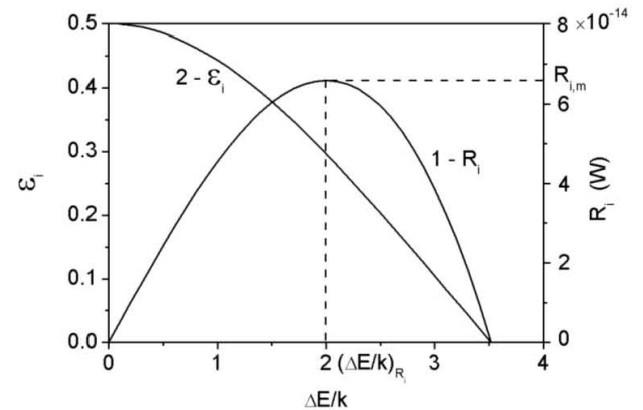


FIGURE 5. Characteristic curves of cooling load  $R_i$  and COP  $\varepsilon_i$  versus resonance width  $\Delta E/k$  characteristics in the intermediate regime.

intermediate regime are studied in this paper. In the analysis, heat transfer of the energy filter via the propagation of phonons is taken into account. The analytical formulae for cooling load and COP of the ESE refrigerator are derived for the two regimes. Numerical results show that, in the maximum cooling load operation regime, due to the existence of energy filter heat conduction, the characteristic curve of cooling load versus COP changes from a monotonic one (without filter heat conduction) to a parabolic-like one (with filter heat conduction), while in the intermediate regime, the characteristic curves of cooling load versus COP are loop-shaped ones and the heat conduction of the filter does not change the shape of the characteristic curves. The cooling load is a parabolic-like function of resonance width while the COP is a monotonic one of resonance width. It is also indicated that, in both

regimes, the COP decreases with the increase in filter heat conduction. The results obtained herein are of great significance for the understanding of thermodynamic performance of the micro-nano thermionic and thermoelectric devices.

## Acknowledgments

This paper is supported by Program for New Century Excellent Talents in the University of P.R. China (Project No. NCET-04-1006) and The Foundation for the Author of National Excellent Doctoral Dissertation of P.R. China (Project No. 200136). The authors wish to thank the reviewer for his careful, unbiased and constructive suggestions, which led to this revised manuscript.

1. G.D. Mahan, *Solid State Physics* **51** (1997) 81.
2. F.J. DiSalvo, *Science* **285** (1999) 703.
3. C. Wood, *Rep. Prog. Phys.* **51** (1988) 459.
4. G. Min and D.M. Rowe, *Solid-State Electronics* **43** (1999) 923.
5. T.C. Harman, P.J. Taylor, M.P. Walsh, and B.E. LaForge, *Science* **297** (2002) 2229.
6. G. Min and D.M. Rowe, *Appl. Energy* **83** (2006) 133.
7. G.N. Hatsopoulos and E.P. Gyftopoulos, *Thermionic Energy Conversion-Vol I: Processes and Devices* (Cambridge: MIT Press, 1973).
8. G.D. Mahan, *J. Appl. Phys.* **76** (1994) 4362.
9. A. Shakouri and J.E. Bowers, *Appl. Phys. Lett.* **71** (1997) 1234.
10. G.D. Mahan and L.M. Woods, *Phys. Rev. Lett.* **80** (1998) 4016.
11. C.B. Vining and G.D. Mahan, *J. Appl. Phys.* **86** (1999) 6852.
12. M.D. Ulrich, P.A. Barnes, and C.B. Vining, *J. Appl. Phys.* **90** (2001) 1625.
13. D. Vashaee and A. Shakouri, *Phys. Rev. Lett.* **92** (2004) 106103.
14. T.E. Humphrey, M.F. O'Dwyer, and H. Linke, *J. Phys. D: Appl. Phys.* **38** (2005) 2051.
15. M.F. O'Dwyer, T.E. Humphrey, R.A. Lewis, and C. Zhang, *J. Phys. D: Appl. Phys.* **39** (2006) 4153.
16. M.F. O'Dwyer, R.A. Lewis, and C. Zhang, *J. Phys. D: Appl. Phys.* **40** (2007) 1167.
17. R.D. Astumian, *Science* **276** (1997) 917.
18. I. Derényi and R.D. Astumian, *Phys. Rev. E* **59** (1999) 6219.
19. T. Hondou, and K. Sekimoto, *Phys. Rev. E* **62** (2000) 6021.
20. M. Asfaw and M. Bekele, *Eur. Phys. J. B* **38** (2004) 457.
21. P. Reimann, *Phys. Rep.* **361** (2002) 57.
22. C. Van den Broeck and R. Kawai, *Phys. Rev. Lett.* **96** (2006) 210601.
23. M. van den Broek and C. Van den Broeck, *Phys. Rev. Lett.* **100** (2008) 130601.
24. G.D. Mahan J.O. Sofo, and M. Bartkowiak, *J. Appl. Phys.* **83** (1998) 4683.
25. G.S. Nolas, J. Sharp, and H.J. Goldsmid, *Thermoelectrics: Basic Principles and New Materials Developments* (Berlin: Springer, 2001).
26. T. Hondou and K. Sekimoto, *Phys. Rev. E* **62** (2000) 6021.
27. J.M.R. Parrondo and B. Jiménez de Cisneros, *Appl. Phys. A* **75** (2002) 179.
28. P. Reimann, M. Grifoni, and P. Hänggi, *Quantum ratchets. Phys. Rev. Lett.* **79** (1997) 10.
29. P. Reimann, *Phys. Rep.* **361** (2002) 57.
30. H. Linke *et al.*, *Science* **286** (1999) 2314.
31. S. Yukawa, G. Tatara, M. Kikuchi, and H. Matsukawa, *Quantum ratchet. Physica B* **284** (2000) 1896.
32. V.S. Khrapai, S. Ludwig, J.P. Kotthaus, H.P. Tranitz, and W. Wegscheider, *Phys. Rev. Lett.* **97** (2006) 176803.
33. V.S. Khrapai, S. Ludwig, J.P. Kotthaus, H.P. Tranitz, and W. Wegscheider, *Phys. Rev. Lett.* **99** (2007) 096803.
34. E.A. Hoffmann and H. Linke, *J. Low Temp. Phys.* **154** (2009) 161.
35. H. Linke *et al.*, *Europhys. Lett.* **44** (1998) 341.
36. H. Linke *et al.*, *Europhys. Lett.* **45** (1999) 406.
37. H. Linke *et al.*, *Phys. Rev. B* **61** (2000) 15914.
38. T.E. Humphrey, H. Linke, and R. Newbury, *Physica E* **11** (2001) 281.
39. H. Linke *et al.*, *Appl. Phys. A* **75** (2002) 237.
40. H. Linke, T.E. Humphrey, R.P. Taylor, A.P. Micolich, and R. Newbury, *Physica B* **314** (2002) 464.
41. T.E. Humphrey, R. Newbury, R.P. Taylor, and H. Linke, *Phys. Rev. Lett.* **89** (2002) 6801.
42. T.E. Humphrey, *Ph. D. Thesis* (University of New South Wales, Australia, 2003).
43. B. Andresen, R.S. Berry, M.J. Ondrechen, and P. Salamon, *Acc. Chem. Res.* **17** (1984) 266.
44. A. Bejan, *J. Appl. Phys.* **79** (1996) 1191.

45. R.S. Berry, V.A. Kazakov, S. Sieniutycz, Z. Szwast, and A.M. Tsirlin *Thermodynamic Optimization of Finite Time Processes* (Chichester: Wiley, 1999).
46. L. Chen, C. Wu, and F. Sun, *J. Non-Equilib. Thermodyn.* **24** (1999) 327.
47. C. Wu, L. Chen, and J. Chen, *Recent Advances in Finite Time Thermodynamics*. (New York: Nova Science Publishers, 1999) p. 560.
48. L. Chen and F. Sun, *Advances in Finite Time Thermodynamics: Analysis and Optimization* (New York: Nova Science Publishers, 2004) p. 240.
49. L. Chen, *Finite-Time Thermodynamic Analysis of Irreversible Processes and Cycles*. (Higher Education Press, Beijing, 2005) p. 280.
50. W. Muschik and K.H. Hoffmann, *J. Non-Equilib. Thermodyn.* **31** (2006) 293.
51. M. Feidt, *Int. J. Exergy* **5** (2008) 500.
52. S. Sieniutycz and J. Jezowski, *Energy Optimization in Process Systems* (Elsevier, Oxford, UK, 2009).
53. S. Velasco, J.M.M Roco, A. Medina, and A.C. Hernández, *J. Phys. D: Appl. Phys.* (2001) **34** 1000.
54. Z.C. Tu, *J. Phys. A: Math. Theor.* **41** (2008) 312003.
55. B.Q. Ai, H.Z. Xie, D.H. Wen, X.M. Liu, and L.G. Liu, *Eur. Phys. J. B* **48** (2005) 101.
56. T. Schmiedl and U. Seifert, *Europhys. Lett.* **81** (2008) 20003.
57. B. Lin and J. Chen, *J. Phys. A: Math. Theor.* **42** (2009) 075006.
58. M. Esposito, K. Lindenberg, and C. Van den Broeck, *Europhys. Lett.* **85** (2009) 60010.
59. F.L. Curzon and B. Ahlborn, *Am. J. Phys.* **43** (1975) 22.
60. J.Z. He, X.M. Wang, and H.N. Liang, *Phys. Scr.* **80** (2009) 035701.
61. X. Fan *et al. Appl. Phys. Lett.* **78** (2001) 1580.
62. D. Vashaee and A. Shakouri, *J. Appl. Phys.* **95** (2004) 1233.
63. M.F. O'Dwyer, R.A. Lewis, C. Zhang, and T.E. Humphrey *Phys. Rev. B* **72** (2005) 205330.
64. T.E. Humphrey, M.F. O'Dwyer, C. Zhang, and R.A. Lewis, *J. Appl. Phys.* **98** (2005) 026108.
65. T.E. Humphrey and H. Linke, *Phys. Rev. Lett.* **94** (2005) 096601.
66. M.F. O'Dwyer, T.E. Humphrey, and H. Linke, *Nanotechnology* **17** (2006) S338.
67. M.F. O'Dwyer, T.E. Humphrey, R.A. Lewis, and C. Zhang *J. Phys. D: Appl. Phys.* **42** (2009) 035417.
68. G. Chen and A. Shakouri, *J. Heat Transfer* **124** (2002) 242.
69. S.T. Huxtable *et al. Appl. Phys. Lett.* **80** (2002) 1737.
70. W. Kim *et al. Appl. Phys. Lett.* **88** (2006) 242107.
71. A. Bejan, *Int. J. Heat Mass Transfer* **31** (1988) 1211.
72. A. Bejan, *Int. J. Heat Mass Transfer* **32** (1989) 1631.